Science of the Total Environment 656 (2019) 1091–1101

Contents lists available at ScienceDirect

Science of the Total Environment

journal homepage: www.elsevier.com/locate/scitotenv

The passion fruit liana (*Passiflora edulis* Sims, Passifloraceae) is tolerant to ozone

Francine Faia Fernandes [a,*], Marisia Pannia Esposito [a], Marcela Regina Gonçalves da Silva Engela [a], Poliana Cardoso-Gustavson [b], Claudia Maria Furlan [c], Yasutomo Hoshika [d], Elisa Carrari [d], Giada Magni [d], Marisa Domingos [a], Elena Paoletti [d]

[a] Instituto de Botânica, Núcleo de Pesquisa em Ecologia, Miguel Stéfano Ave. 3687, 04045-972 SP, Brazil
[b] Universidade Federal do ABC, Centro de Ciências Naturais e Humanas, Arcturus St. 03, 09606-070 SBC, Brazil
[c] Universidade de São Paulo, Instituto de Biociências, Matão St. 257, 05508-090 SP, Brazil
[d] National Research Council (CNR), Via Madonna del Piano 10, 50019 Sesto Fiorentino, Italy

HIGHLIGHTS

- Seedlings of *Passiflora edulis* were exposed to ozone in a FACE system.
- Anatomical changes observed in leaf tissue may restrain damage progression.
- A high level of O_3 did not affect physiological processes.
- Biochemical leaf traits enable *P. edulis* to tolerate oxidative stress.
- *P. edulis* can be considered an O_3-tolerant species.

GRAPHICAL ABSTRACT

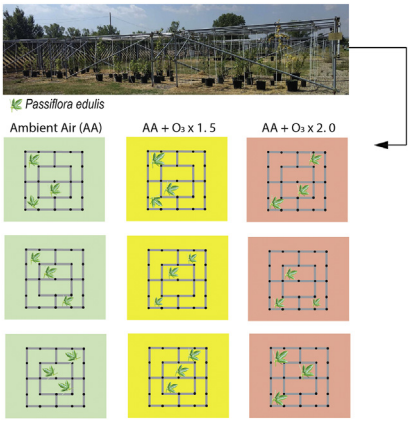

ARTICLE INFO

Article history:
Received 1 October 2018
Received in revised form 23 November 2018
Accepted 28 November 2018
Available online 30 November 2018

Editor: Pavlos Kassomenos

Keywords:
Anatomical acclimatization
Antioxidant system
Liana
Oxidative stress
Polyphenols

ABSTRACT

Passiflora edulis Sims is a liana species of high economic interest and is an interesting model plant for understanding ozone action on disturbed vegetation. In this work we hypothesized that *P. edulis* has adaptive responses to oxidative stress that enable it to tolerate ozone damage based on its capacity to grow under a diversity of environmental conditions and to dominate disturbed areas. We exposed seedlings to three levels of ozone in a Free-Air Controlled Exposure (FACE) system (22, 41 and 58 ppb h AOT40 and 13.52, 17.24 and 20.62 mmol m^{-2} POD0, over 97 days) for identifying its tolerance mechanisms. Anatomical (leaf blade structure and fluorescence emission of chloroplast metabolites), physiological (leaf gas exchange, growth rate and biomass production) and biochemical (pigments, total sugars, starch, enzymatic and non-enzymatic antioxidant metabolites, reactive oxygen species and lipid peroxidation derivatives) responses were assessed. Ozone caused decreased total number of leaves, hyperplasia and hypertrophy of the mesophyll cells, and accelerated leaf senescence. However, O_3 did not affect carbohydrates content, net photosynthetic rate, or total biomass production, indicating that the carboxylation efficiency and associated physiological processes were not affected. In addition, *P. edulis* showed higher leaf contents of ascorbic acid, glutathione (as well high ratio between their reduced and total forms), carotenoids, and flavonoids located in the chloroplast outer envelope membrane.

* Corresponding author.
E-mail addresses: fernandes.francinef@gmail.com, franzinha.fernandes@gmail.com (F.F. Fernandes).

https://doi.org/10.1016/j.scitotenv.2018.11.425
0048-9697/

Tropical environment
Vine species

Our results indicate that *P. edulis* is an O_3-tolerant species due to morphological acclimation responses and an effective antioxidant defense system represented by non-enzymatic antioxidants, which maintained the cellular redox balance under ozone.

1. Introduction

Lianas – climbing vines with woody stems – are a key component of most tropical forests due to their abundance, constituting 10% to 45% of the woody species (Pivello et al., 2018). They are also the second life-form in biomass production after trees (DeWalt and Chave, 2004; Pérez-Salicrup et al., 2004). They ascend in suitable hosts, and live for decades, occurring also in mid-to-late successional forests (Rossell and Eggleston, 2017). When present in a high density, they may further reduce tree growth and alter tree species composition, changing the forest physiognomy and reducing the capacity of forests to sequester atmospheric carbon (Phillips et al., 2002; Schnitzer and Bongers, 2002; Pivello et al., 2018). It is thus important to predict the reasons of the high abundance of lianas in tropical forests (Schnitzer, 2005; Pivello et al., 2018). The high capacity of hydraulic redistribution and water storage, multifocal growth, drought resilience and acquisitive resource syndrome are among them (Amorim et al., 2018).

Passiflora is the largest genus of Passifloraceae, comprising about 520 species (Wohlmuth et al., 2010) predominantly found in tropical and subtropical regions (Dhawan et al., 2004; Araújo et al., 2017). Its distribution is directly determined by the environmental conditions, such as seasonality in temperature and rain precipitation (Scherer, 2014). Brazil is the hotspot in Passifloraceae biodiversity, including *Passiflora edulis* Sims, which is distributed in heterogeneous environments and in different phytogeographic domains (Scherer, 2014; Flora do Brasil 2020, under construction). In addition, *P. edulis* shows a higher ability to adapt and acclimate to drought than other *Passiflora* species, as reported in a controlled experiment (Souza et al., 2018).

Tropospheric ozone (O_3) is a strong oxidizing air pollutant formed through a complex series of reactions involving the action of sunlight on nitrogen dioxide and hydrocarbons (Ashmore, 2005; Lodovici and Bigagli, 2011). The tolerance level of plants to O_3 depends on their absorption rate, constitutive detoxification capacity (enzymatic and non-enzymatic antioxidant metabolites), carboxylase ratio and capacity of antioxidant regeneration (Matyssek et al., 2012). After entrance, O_3 reacts with water, leading to the formation of reactive oxygen species (ROS) at the interface of cell wall. The oxidative destruction of lipids and proteins of the plasma membrane and production of other free radicals and reactive intermediates, is a process known as lipid peroxidation (Kanofsky and Sima, 2005; Puckette et al., 2007). Since the half-lives of mostly ROS are extremely short, stable end products of oxidative damage in cell macromolecules are used to measure the oxidative stress (Bhaduri and Fulekar, 2012). ROS may cause oxidative lesions that result in anatomical leaf changes (Vollenweider et al., 2003), and in negative impacts on plant metabolism and photosynthesis that may progress to the appearance of visible leaf O_3 injury and reduction of plant growth and development (Hernandez-Gimenez et al., 2002; Matyssek and Sandermann, 2003).

We assumed that *P. edulis* is an interesting model species for understanding O_3 action on disturbed vegetation, given its wide distribution in the tropics (Flora do Brasil 2020, under construction) and its high abundance in disturbed vegetation by human action, where high O_3 levels are expected. Considering its vine characteristics above mentioned that enable it to tolerate natural environmental stresses, we raised the hypothesis that *P. edulis* also has adaptive responses that enable it to tolerate the oxidative stress caused by O_3. The knowledge on the tolerance level of *P. edulis* to O_3 is also of economic interest because several *Passiflora* species are widely cultivated in tropical and subtropical regions. The fruits of *P. edulis* are, in particular, the most consumed among several species of *Passiflora* in the international market (Ocampo et al., 2010; Souza et al., 2018). In addition, *Passiflora* species have great pharmacological value (Dornelas et al., 2006) because of the bioactive compounds found in the aerial vegetative organs (Otobone et al., 2005; Yudasheva et al., 2005; Castro et al., 2007).

Aiming to test the above mentioned hypothesis, we assessed anatomical (leaf blade structure and fluorescence emission of chloroplast metabolites), physiological, (leaf gas exchange, stomatal ozone uptake, growth rate, biomass production) and biochemical (pigments, primary and secondary metabolites, antioxidants, reactive oxygen species and lipid peroxidation derivatives) responses in plants exposed to ozone in a Free-Air Controlled Exposure (FACE) system.

2. Materials and methods

2.1. Experimental design

Seedlings of *P. edulis* (approx. 20 cm high) were obtained from an Italian nursery (43.935351 N, 10.928174 E) and transplanted to 17 L pots filled with a mixture of sand: peat: nursery soil (1:1:1, v/v). Plants were irrigated every afternoon by a drip irrigation system to avoid water stress (i.e., volumetric soil water content was maintained to the field capacity of ≈0.295 $m^3\ m^{-3}$, Paoletti et al., 2017), and fertilized with N:P:K (10:10:10) every 7 days during the first and second month of exposure, and once in the last month of the experiment.

The experiment was carried out in an O_3 FACE system located in Sesto Fiorentino, Florence, Italy (43°48′59″ N, 11°12′01″ E, 55 m a.s.l.). Details of this experimental facility are given in Paoletti et al. (2017). The plants were submitted to three O_3 levels: ambient air (AA); intermediate ozone level (AA + O_3 × 1.5) and elevated ozone level (AA + O_3 × 2.0) during 97 days of summer season (from June 10th to September 15th, 2017). The system consisted of three plots per O_3 treatment; each plot (5 × 5 × 2 m, L × W × H respectively) was considered as a replicate. Three pots of *P. edulis* were maintained in each plot (n = 3, totalizing nine plants per O_3 treatment = 27 plants).

The O_3 concentration was continuously monitored in one plot per O_3 treatment using monitors (Mod. 202, 2B Technologies, Boulder CO, USA) and the AOT40 (accumulated O_3 exposure over a threshold of 40 ppb) was calculated during daylight hours (global radiation > 50 W m^{-2}), following the protocol described in CLRTAP (2017). Global solar radiation (GSR), temperature (Temp), relative humidity (RH) and precipitation (P) were continuously recorded during the experiment by a Watchdog station (Mod. 2000; Spectrum Technology, Inc., Aurora, IL, USA) at 2.5 m a.g.l.

2.2. Anatomical responses

Samples for microscopic evaluation were gathered on leaves collected at the end of the experiment. We sampled symptomatic leaves (chlorosis induced by O_3, as shown in Fig. S1 of the Supplementary material) of plants from all treatments and asymptomatic leaves only of plants from the AA treatment. Fragments (approx. 1 cm^2) of the median region of both asymptomatic and symptomatic leaves were fixed in 2.5% glutaraldehyde buffered at pH 7.0 with 0.067 M Sorensen phosphate buffer, and placed under vacuum before storing at 4 °C.

Part of the fragments destined to confocal analyses (Zeiss LSM 510-Meta) were washed in distilled water, cut at 20 μm thickness by a cryomicrotome (Leica CM1100), and mounted in Fluoromount (Sigma-Aldrich) aqueous medium. The samples were excited with a

364 nm laser to promote polyphenol (Fernandes et al., 2016) and carotenoid emissions (Roshchina, 2008; D'Andrea et al., 2014). Emissions were taken from 400 to 607 nm and subsequently from 400 to 700 nm in a lambda stack mode (a series of images from the same microscopic region with different wavelengths with 10 to 11 nm increments) for better visualization of chloroplast metabolites. In each image (objective lens 40×), six chloroplasts of the palisade parenchyma were randomly selected and the intensities of metabolite emission in the obtained spectra (400–607 nm and 400–700 nm) were quantified using the software Zeiss LSM Image Browser. The emission wavelength (nm) between 450 and 500 nm referred to phenolic compounds, 500–550 nm to carotenoids, and above 650 nm to chlorophylls (chl *a* and *b*).

The other part of the fragments was dehydrated in an ethanol series, embedded in Technovit 7100 historesin and transversally sectioned to 1.5 μm semi-thin cuttings by a rotary microtome Leica (RM2245) for structural and histochemical analyses. Material was stained with toluidine blue and *p*-phenylenediamine for metachromasy and lipid identification, respectively (Feder and O'Brien, 1968; Kivimäenpää et al., 2004), PAS reaction for polysaccharides (Gahan, 1984) and Comassie blue for proteins (Wetzel et al., 1989).

2.3. Physiological responses

2.3.1. Leaf gas exchange and stomatal ozone uptake (POD)

Gas exchange measurements of fully expanded sun leaves (4th to 6th from the shoot tip) were carried out by a portable infrared gas analyzer (CIRAS-2 PP Systems, Herts, UK). On 11–14th September, the measurements were taken with a control value of photosynthetic photon flux density (PPFD) of 1500 μmol m^{-2} s^{-1}, ambient CO_2 concentration (Ca) of 400 μmol mol^{-1}, relative humidity of 40 to 60% and leaf temperature of 25 °C, from 9:00 to 12:00 h. We determined the light-saturated net photosynthetic rate (A_{sat}), stomatal conductance for water vapour (g_{sw}) and intercellular CO_2 concentration (Ci) at ambient CO_2 concentration (400 ppm) for calculating the Ci/Ca ratio.

The O_3 dose during the experiment was calculated as phytotoxic ozone dose (POD_Y) above an hourly stomatal uptake threshold of 0 nmol m^{-2} s^{-1} (POD_0). POD_Y is given as follows:

$$POD_Y = \sum \max(F_{st} - Y,\ 0) \quad (1)$$

where F_{st} is an hourly mean stomatal O_3 uptake (nmol m^{-2} s^{-1}) and Y is a species-specific threshold of stomatal O_3 uptake (nmol m^{-2} s^{-1}). As it was not clear which threshold Y can be applied to this species, we did not set a threshold i.e. Y = 0 (POD_0) in the present study. F_{st} was calculated according to CLRTAP (2017), as follows:

$$F_{st} = [O_3] \cdot g_s \cdot \frac{r_c}{r_b + r_c} \quad (2)$$

where $[O_3]$ is the hourly O_3 concentration (ppb), g_s is the stomatal conductance for O_3 (m s^{-1}), r_c is the leaf surface resistance ($r_c = 1 / (g_s + g_{ext})$, where $g_{ext} = 0.0004$ m s^{-1} indicates a cuticular and/or external leaf conductance), and r_b is the leaf boundary layer resistance (m s^{-1}). Stomatal conductance was estimated by the multiplicative empirical model (Jarvis, 1976; CLRTAP, 2017; Hoshika et al., 2018). The detail is described in the Supplementary file.

2.3.2. Growth rate and biomass production

Growth characteristics were monthly assessed by measuring plant height, stem diameter (near the base) and total number of leaves. The measuring times were referred as T0 (initial measurement) to T3 (final measurement). For the determination of stem height and diameter, a measuring tape and a digital caliper (data expressed in cm) (Digimess, São Paulo, Brazil) were used (Sá et al., 2014), respectively. Relative growth rate (RGR) was calculated every month in relation to the previous measurement (T1 − T0; T2 − T1 and T3 − T2) and also between the initial and final measurements (T3 − T0), using the formula proposed by Benincasa (1988).

At the end of the exposure period, leaves, stems/branches and roots of each plant were harvested, stored in paper packaging and dried in an oven at 60 °C until constant weight. The leaf, stem/branch and root biomasses of an additional lot of 5 plants were determined at the beginning of the experiment in order to obtain the T0 values. Shoot to root ratios were calculated according to Moura et al. (2017).

2.4. Biochemical responses

The biochemical responses were measured on a composite sample of four fully-expanded and sun-exposed leaves per plant, according to the methods described below. The composite leaf samples were stored in an ultra-freezer, under −80 °C. For biochemical responses, three analytical replicates were performed in asymptomatic leaf samples.

2.4.1. Pigments

The pigment Chl *a* and *b* and carotenoids (CAR) content was determined in the same leaf extracts by spectrophotometric UV–vis method. The extracts were obtained by homogenizing frozen leaves in ethanol (96%). The supernatant was measured at 470 nm to determine the levels of carotenoids, at 649 nm to determine Chl *a* and at 666 nm to determine Chl *b* (Wintermans and De Mots, 1965).

2.4.2. Primary and secondary metabolites

Total carbohydrate contents in the frozen leaf samples (100 mg) were extracted in 80% ethanol and determined colorimetrically at 490 nm using the phenol–sulfuric acid method (Dubois et al., 1956). Starch content was determined by using 10 mg of the freeze-dried residue after ethanol extraction. The absorbance was measured in an Elisa plate at 490 nm (Amaral et al., 2007).

The total flavonoids were extracted from the frozen leaves (100 mg) with 80% methanol in dry bath (at 70 °C for 1 h). The amounts of total flavonoids were quantified using aluminum chloride 5% method at 420 nm (Santos and Furlan, 2013).

2.4.3. Antioxidants

Ascorbic acid, in its reduced (AsA) and total (totAA) forms, was analyzed in frozen leaves using the chromatographic method described by López et al. (2005) and a HPLC (Metrohm) connected to an UV–Vis detector.

Glutathione in its reduced (GSH), oxidized (GSSG) and total (totG) content was determined in frozen leaves according to the method described by Israr et al. (2006).

Superoxide dismutase (SOD), ascorbate peroxidase (APX) and catalase (CAT) activities were analyzed by spectrophotometric UV–vis using extracts of frozen leaves. SOD and APX activities were determined according to a slightly modified version of the method described by Reddy et al. (2004). CAT activity was determined as described by Kraus et al. (1995) with some modifications proposed by Azevedo et al. (1998). The activity of glutathione reductase (GR) was determined in frozen leaves according to the method of Reddy et al. (2004).

Further analytical details about enzymatic and non-enzymatic compounds can be found in Esposito et al. (2016).

2.4.4. Reactive oxygen species, malondialdehyde and hydroperoxide conjugated diene

The principle of the •OH radical assay was the quantification of the 2-deoxyribose degradation product, malondialdehyde (MDA), by its condensation with thiobarbituric acid (TBA). The reactions started by the addition of Fe (II) to solutions containing 2-deoxyribose, iron chelator, phosphate buffer (pH = 7.2) and then were stopped by the addition of phosphoric acid followed by TBA. The absorbance of this mixture was measured at 532 nm (Lopes et al., 1999).

The H_2O_2 contents were determined following Alexieva et al. (2001). The reaction mixture consisted of supernatant extract (frozen leaves + trichloroacetic acid), potassium phosphate buffer (100 mM, pH 7.0) and reagent potassium iodide (KI). The reaction was developed for 1 h in darkness and absorbance was measured at 390 nm.

The $O_2^{\bullet -}$ production rate was determined using the hydroxylamine oxidation method (Wang and Luo, 1990) with some modifications. The supernatant was mixed with potassium phosphate buffer (pH 7.8) and hydroxylamine chloride. *p*-Aminobenzene sulfonic acid, α-naphthylamine and *n*-butyl alcohol were added and the final supernatant was used for measuring absorbance at 530 nm.

The concentrations of MDA were determined following the method proposed by Hodges et al. (1999) with the corrected equation proposed by Landi (2017) and concentrations of hydroperoxide conjugated diene (HPCD) were obtained from frozen leaves in ethanol (96%) by spectrophotometric UV–Vis method. The absorbance was measured at 234 nm (Levin and Pignata, 1995).

Further analytical details about ROS and indicators of oxidative stress can be found in Esposito et al. (2018).

2.5. Statistics

The significant differences between the treatments relative to fluorescence emission of chloroplast metabolites, physiological and biochemical responses and relative growth rates between the initial and final measurements (T3 − T0) were determined by one-way ANOVA. When necessary, the data were transformed to reach normal distribution and equal variances. The Holm-Sidak method was employed to identify significant differences between the three treatments (AA, AA + O_3 × 1.5 and AA + O_3 × 2.0). The significant differences in monthly relative growth rates (RGR) were tested by two-way ANOVA with repeated measures (factor 1: O_3 treatment; factor 2: measurement time). After testing the interaction of both factors, the Holm-Sidak method was employed to identify significant differences between the three treatments and different measurement times. Results were considered significant at $p < 0.05$.

3. Results

3.1. Environmental conditions during the experimental period

During the experimental period, the average daily (24 h) air temperature varied between 19 and 32 °C and daily maximum hourly values varied between 21 and 43 °C (Fig. 1). Average daily GSR was 57–400 W m^{-2} and daily maximum hourly values were 927–1186 W m^{-2}. Total daily precipitation varied between 0 and 62 mm, and average daily relative humidity was 23–85%. The mean daily O_3 concentrations (24 h) varied between 17 and 71 ppb at AA, 23 and 91 ppb at AA + O_3 × 1.5 ppb and 28 and 111 ppb at AA + O_3 × 2.0 (Fig. 1). After 97 days of exposure, AOT40 reached 22, 41 and 58 ppm h at AA, AA + O_3 × 1.5 and AA + O_3 × 2.0 treatments, respectively.

3.2. Anatomical responses

The asymptomatic leaf blade of AA plants showed uniseriated epidermis and thin cuticle. The leaf blade had a uniseriate hypostomatic epidermis and a thin cuticle. The mesophyll was dorsiventral with one layer of palisade parenchyma and 4–5 layers of spongy parenchyma cells. The parenchyma cells showed thin cell walls, peripheral flattened chloroplasts with starch grains, hyaline vacuole and pronounced intercellular spaces (Fig. 2A–D). A strong reaction to total proteins stain was observed in the chloroplasts (Fig. 2E).

Symptomatic leaves from intermediate and elevated levels of O_3 (AA + O_3 × 1.5 and AA + O_3 × 2.0, respectively) showed changes in cell wall of the palisade parenchyma cells, that exhibited a sinuous shape (Fig. 2G). An apparent reduction in the size and density of chloroplasts and changes in their shapes was observed in the palisade cells along the leaf blade (Fig. 2F–H). In addition, the starch grains inside the

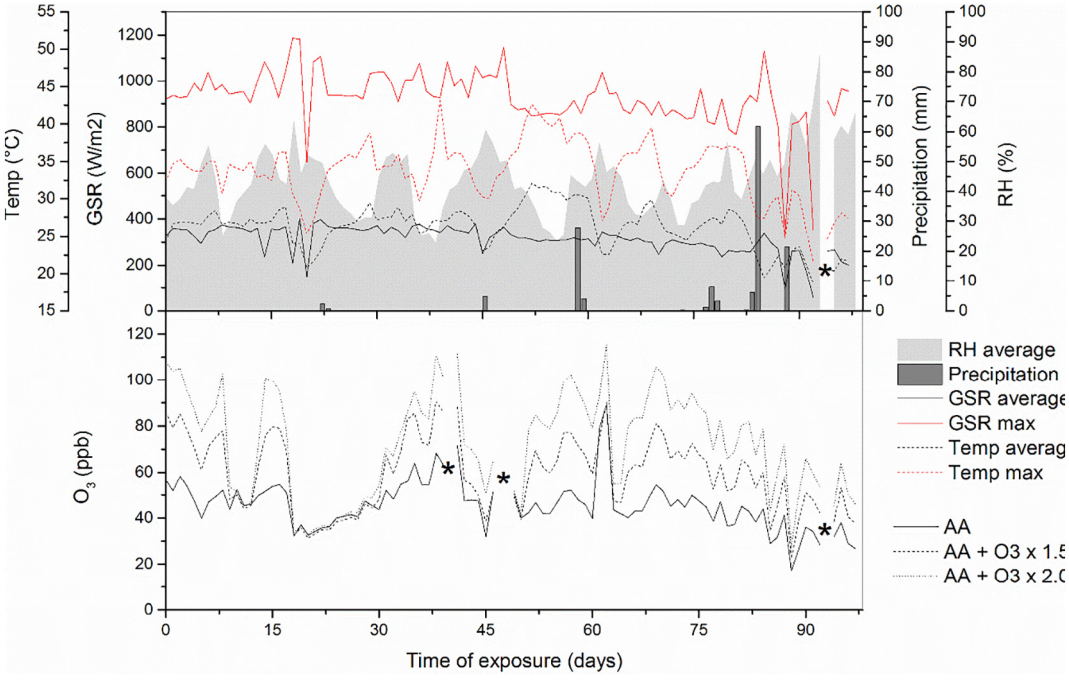

Fig. 1. Environmental conditions over the experimental period (from June 10th to September 15th, 2017 = 97 days of exposure). (*) indicates the absence of data. Daily average of temperature (Temp average), relative humidity (RH average), global solar radiation (GSR average), ozone concentrations at ambient air (AA), intermediate ozone level (AA + O_3 × 1.5) and elevated ozone level (AA + O_3 × 2.0) and total daily precipitation (P). Daily maximum of temperature (Temp max) and global solar radiation (GSR max).

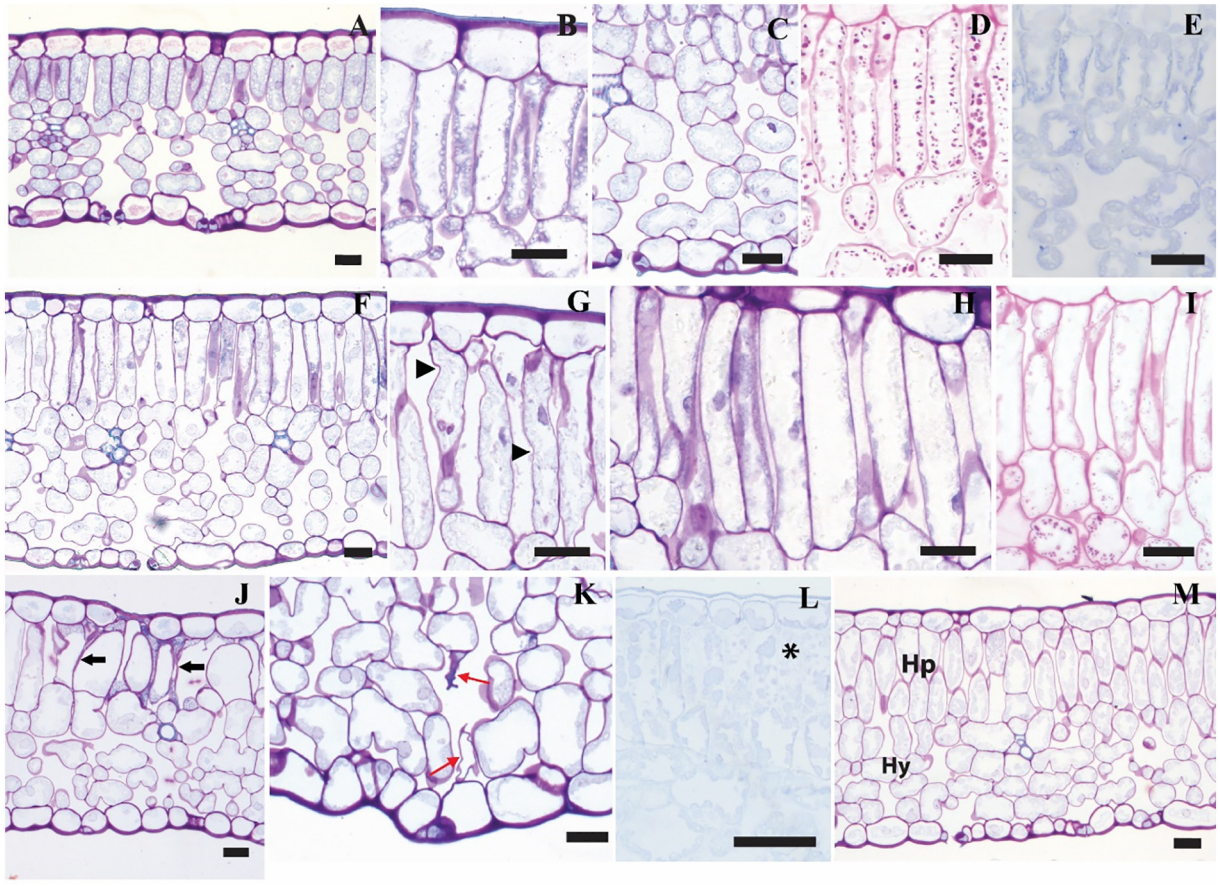

Fig. 2. Structural aspects of *P. edulis* leaves from ambient air (A–E) and from ozone treatments (AA + O_3 × 1.5 and AA + O_3 × 2.0) (F–M). Parenchyma cells with thin cell walls, hyaline vacuole and pronounced intercellular spaces (A). Flattened chloroplasts diffusely distributed in the palisade parenchyma (B) and spongy parenchyma cells (C). Starch grains inside the chloroplasts (D). A strong reaction to total proteins stain inside the chloroplasts (E). An apparent reduction in the amount, size and density of chloroplasts along the leaf blade (F–H). Changes in cell wall and chloroplasts shape (arrowheads, G). Chloroplasts do not accumulate starch grains (I). Collapse of palisade (arrows, J) and spongy parenchyma cells close to stomata (red arrows, K). Weak reaction to protein stain. Proteins accumulated in the protoplast (black asterisk, L). Hyperplasia of palisade parenchyma (Hp) and hypertrophy (Hy) of spongy parenchyma cells in AA + O_3 × 2.0 (M). Toluidine blue (A–C, F–H, J–L, M); PAS test, total polysaccharides (D and I); Coomassie blue, total proteins (D and L). Bars = 25 μm.

chloroplasts in the parenchyma palisade were smaller or absent (Fig. 2I). Small groups of collapsed cells were observed in the palisade (Fig. 2J) and spongy parenchyma (Fig. 2K). A weaker reaction to protein stain and a positive reaction in the protoplast were observed in O_3–exposed leaves compared to AA (Fig. 2E vs L).

The symptomatic leaves from AA + O_3 × 2.0 showed reductions of intercellular spaces resulting from hyperplasia of palisade parenchyma, identified as an increase in the number of cell layers, and hypertrophy of spongy parenchyma, characterized by an increase in its cell size (Fig. 2O).

Asymptomatic leaves exhibited low emission intensity of constitutive flavonoids located in the outer envelope membrane (OEM) and of carotenoids, with the emission intensity of carotenoids higher than that of OEM-flavonoids (Fig. 3A). There was also a low emission intensity of pheophytins (Fig. 3A). In addition, a high emission intensity of chlorophylls (>650 nm) was observed regardless of the region of interest (ROI) selected for analysis (Fig. 3B). In contrast, symptomatic samples from ozone treatments (AA + O_3 × 1.5 and AA + O_3 × 2.0) had an increase of the emission intensity of flavonoids, carotenoids, pheophytins and lipofuscins-like (Fig. 3C). The chlorotic cells did not exhibit chlorophyll emission, while adjacent chlorotic cells (ROI 2) exhibited a similar emission intensity pattern as the one observed in the AA samples (Fig. 3D). The emission intensity of lipofuscin-like and OEM flavonoids in the chloroplasts were significantly higher in the samples from treatments with intermediate and elevated levels of O_3 when compared to those from the AA treatment (Fig. 3E). Although the emission intensity of carotenoids in leaf samples from the treatments with ozone was higher than that obtained in the AA treatment, only the results from the AA + O_3 × 1.5 differed significantly from the AA treatment (Fig. 3E). There were no significant differences between treatments in terms of chlorophyll and pheophytin emission intensities (Fig. 3E).

3.3. Physiological and biochemical responses

3.3.1. Leaf gas exchange

One-way ANOVA revealed that the light-saturated net photosynthetic rate (A_{sat}) of *P. edulis* leaves did not differ significantly among O_3 treatments (Table 1). Stomatal conductance (g_{sw}) and the Ci/Ca ratio were not statistically different among O_3 treatments. POD0 varied between 13.52 mmol m^{-2} at AA, 17.24 mmol m^{-2} at AA + O_3 × 1.5 and 20.62 mmol m^{-2} at AA + O_3 × 2.0 treatments.

3.3.2. Relative growth rates

The interacting effects of both factors (O_3 treatment and time of measurement) on the relative growth rates (RGR) were not significant for any growth parameter ($p > 0.05$). The elevated O_3 level (AA + O_3 × 2.0) reduced the RGR in leaf number during all time intervals in comparison to the other treatments. No significant effect of O_3 was proved on the RGR in diameter. However, in relation to RGR in height, significant differences were found among times of measurement. In general, lower RGRs were observed during the last month of experiment (T3 and T2) for all parameters (Fig. 4).

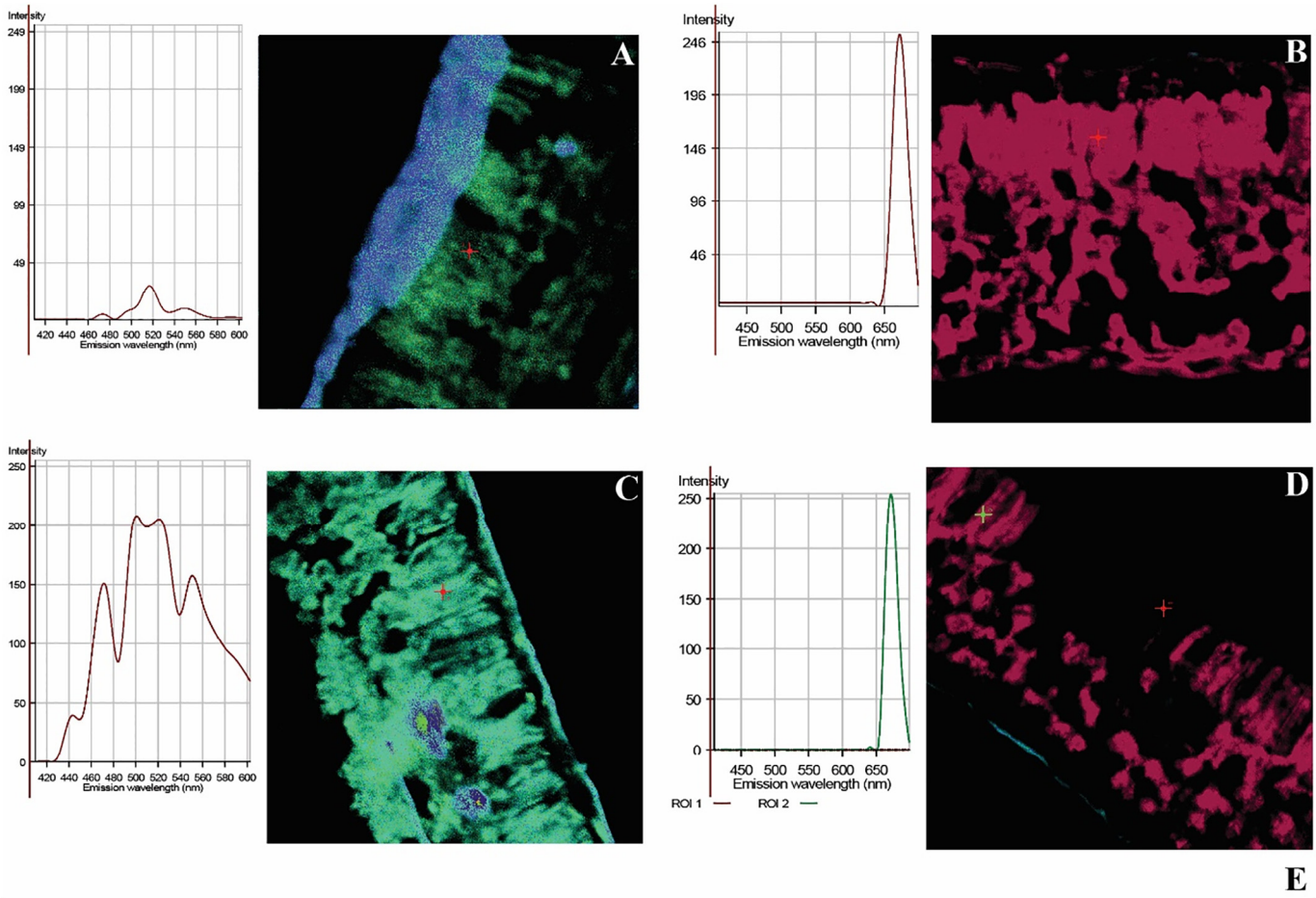

E

treatment	lipofuscins (intensity- nm)	flavonoids (intensity- nm)	carotenoids (intensity -nm)	pheophytins (intensity- nm)	clorophyll (intensity- nm)
AA	0.77 (±1.13) b	18.01 (± 16.38) b	60.38 (±22.61) b	20.63 (± 16.21) a	107.83 (± 14.32) a
AA + O_3 x 1.5	5.38 (± 0.98) a	75.52 (± 9.88) a	126.35 (± 16.67) a	57.44 (± 13.28) a	54.76 (± 38.09) a
AA + O_3 x 2.0	3.42 (± 1.05) a	55.72 (± 16.77) a	108.5 (± 22.87) ab	46.58 (± 21.85) a	70.96 (± 20.59) a

Fig. 3. Emission spectra of chloroplasts (A–D) and quantification of the emission intensity of chloroplast metabolites (E) in leaves of *P. edulis* from ambient air (AA) (A, B and E) and ozone treatments (AA + O_3 × 1.5 and AA + O_3 × 2.0) (C, D and E). Emission spectra of chloroplasts from AA (regions of interest; ROI 1 in the palisade parenchyma): the peak between 450 and 500 nm refers to flavonoids, 500 and 550 nm to carotenoids and 550 and 600 pheophytins (A). Emission referring only to chlorophyll (above 650 nm; ROI 1 in the palisade parenchyma) from AA (B). Emission spectra of chloroplasts from ozone treatments (C). Note that the peaks related to carotenoids (500–550 nm), flavonoids (450–500 nm) and pheophytins (550–600 nm) increase and appears lipofuscin-like peaks (peak between 400 and 450 nm refers to lipofuscin). Emission referring only to chlorophyll in the palisade parenchyma from ozone treatments (D). Note the absence of chlorophyll emission from some groups of palisade parenchyma cells (ROI 1), while adjacent cells (ROI 2) exhibited. Median values (± standard deviation) of the intensity of lipofuscins, flavonoids, carotenoids, pheophytins and chlorophyll fluorescence emission peaks from chloroplasts (E). Different letters indicate significant differences in each treatment ($p < 0.05$, Holm-Sidak method test, N = 3).

The biomass of leaf, stem and root as well as the shoot to root ratios did not vary significantly among the O_3 treatments (data not shown).

Table 1
Photosynthetic traits (A_{sat}, light-saturated net photosynthetic rate; g_{sw}, stomatal conductance for water vapour; Ci/Ca, ratio of intercellular CO_2 concentration (Ci) to ambient CO_2 concentration) of leaves of *P. edulis* seedlings exposed to three treatments of ozone (AA = ambient air, AA + O_3 × 1.5 = intermediate and AA + O_3 × 2.0 = elevated ozone levels) for 97 days. Data are shown as mean ± S.E. (n = 3). Different letters indicate significant differences between the treatments by Holm-Sidak test ($p < 0.05$), n = 3.

Treatment	A_{sat} (μmol m^{-2} s^{-1})	g_{sw} (mol m^{-2} s^{-1})	Ci/Ca ratio (fraction)
AA	8.8 ± 0.1 a	0.10 ± 0.01 a	0.58 ± 0.03 a
AA + O_3 × 1.5	7.7 ± 0.5 a	0.07 ± 0.01 a	0.49 ± 0.03 a
AA + O_3 × 2.0	6.9 ± 0.6 a	0.07 ± 0.01 a	0.50 ± 0.04 a

3.3.3. Pigments

The chlorophyll *a* content, chlorophyll *a*/*b* ratio and carotenoid content were significantly higher in the treatment with elevated levels of ozone than in AA and AA + O_3 × 1.5 (Table 2).

3.3.4. Primary and secondary metabolites

The leaf content of total sugars did not differ among treatments and the leaf content of starch was significantly higher in the AA + O_3 × 1.5 treatment than in the others (Table 2).

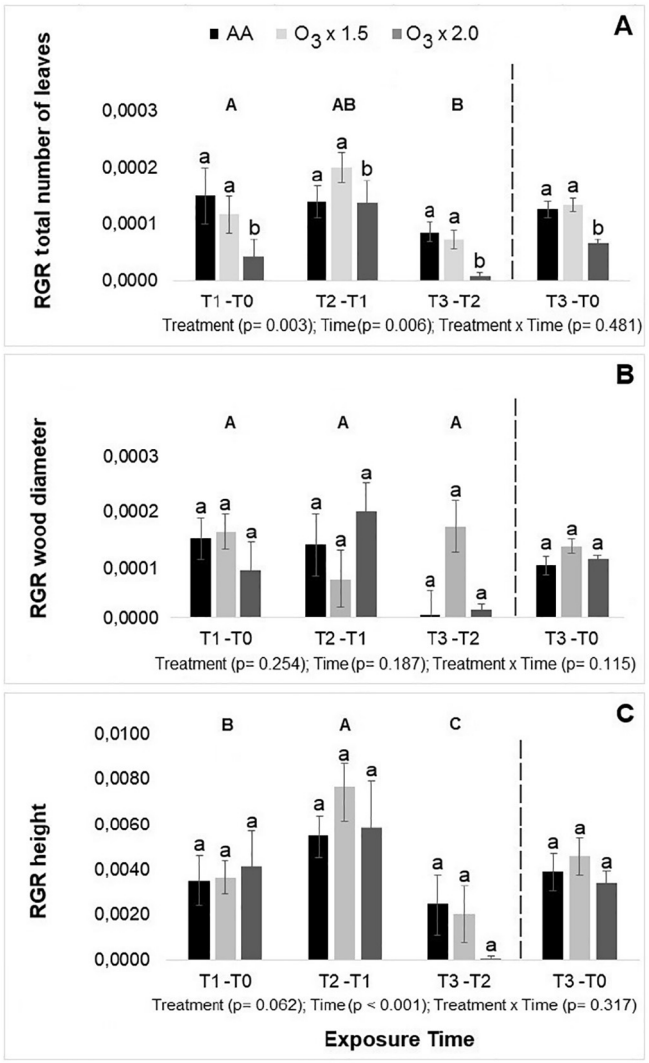

Fig. 4. Relative growth rates (RGR) per day of fumigation between monthly intervals of measurement (T1 — T0, T2 — T1, T3 — T2) and between the initial and final measurements (T3 — T0), of: total number of leaves (A), diameter (B) and height (C) of *P. edulis* plants exposed to three treatments of ozone (AA = ambient air, AA + O_3 × 1.5 = intermediate and AA + O_3 × 2.0 = elevated ozone levels) for 97 days. Different lower case letters indicate significant differences between the treatments during the same monthly interval of measurement. Different upper case letters indicate differences in the RGR between monthly intervals of measurement in the same treatment. $p < 0.05$, Holm-Sidak method, N = 3.

Leaf accumulation of total flavonoids was higher in plants exposed to AA + O_3 × 2.0 and to AA + O_3 × 1.5 than in plants from AA.

3.3.5. Antioxidants

The content of non-enzymatic antioxidants – ascorbic acid and glutathione in their reduced, oxidized and total forms – was significantly enhanced in the treatments with intermediate and elevated levels of ozone when compared to AA treatment (Table 2). There was no difference between the ozone treatments (×1.5 and ×2.0). The redox potential of both ascorbic acid (medians ≥ 0.71) and glutathione (medians ≥ 0.48) was high but did not differ between the ozone treatments. The activity of enzymatic antioxidants – CAT, GR and APX – was significantly higher in the plants grown in the AA treatment than in the plants included in the treatments with ozone addition. The activity of SOD did not differ among the treatments (Table 2).

3.3.6. Reactive oxygen species and lipid peroxidation derivatives

The leaf accumulation of •OH was similar in plants from all treatments, but the $O_2^{\bullet -}$ ion and the H_2O_2 content were higher in the treatments with intermediate and elevated levels of ozone when compared to AA.

The indicators of lipid peroxidation – MDA and HPCD – and flavonoids also increased in the plants included in the treatments with intermediate and elevated levels of ozone when compared to AA treatment (Table 2).

4. Discussion

The occurrence of symptomatic leaves indicated that *P. edulis* plants exposed to high levels of ozone showed injury of leaf cells and tissues. The visible O_3 symptoms were restricted to foliar yellowing, which is generally a consequence of chlorophyll degradation (Günthardt-Goerg and Vollenweider, 2007). The appearance of visible injury is a common symptom observed in vine species exposed to O_3. It was registered for example by Saitanis (2003) in *Vitis vinifera* in Greece, by Manning and Godzik (2004) in *Humulus lupulus* in Central and Eastern Europe and by Ferreira et al. (2012) in *Ipomoea nil* 'Scarlet O'Hara' in the state of São Paulo, Brazil. The confocal analyses indicated a degradation of chlorophylls inside the chloroplasts of chlorotic leaves under elevated ozone levels, compared to chlorophyll emissions in asymptomatic leaves of plants exposed to ambient ozone level. However, such difference was not statistically significant. Peaks related to products of oxidative damage were observed by confocal analyses (lipofuscin-like and pheophytins). Pheophytins are the first product resulting from the degradation of chlorophyll under air pollution (Gowin and Goral, 1977), characterized by the loss of the central Mg of the chlorophyll molecule (Eijckelhoff and Dekker, 1997). Although pheophytin emission increased in symptomatic leaf samples under the ozone treatments, the chlorophyll emission under confocal analysis did not change significantly. The confocal analysis does not distinguish chlorophyll *a* and *b*, as well as pheophytin *a* and *b*. The chlorophyll analysis from asymptomatic leaves revealed an increase in the concentration ratio between chlorophylls *a* and *b* due to enhanced levels of chlorophyll *a* in plants exposed to the highest level of ozone, which explains the non-significant variation in chlorophyll emission in the confocal analyses. These results indicated the conversion of chlorophyll *b* to pheophytins *b* (Xu et al., 2001). In addition, the chl *a*/*b* ratio is very low as compared to commonly observed values in higher plants.

The foliar yellowing and chlorophyll alterations can be indicative of premature foliar senescence in response to ozone (Pell et al., 1997). Accelerated senescence in response to O_3 exposure was observed in the vine *Vitis vinifera* in controlled-exposure experiments (Soja et al., 1997). Accelerated foliar senescence may be one of the explanations for the significantly lower leaf number of *P. edulis* plants under the highest level of O_3. This effect might be considered an avoidance mechanism that restrains the progression of O_3 damage in the plants. This mechanism, together with the anatomical, biochemical and physiological responses discussed below, may contribute to improve O_3 tolerance in *P. edulis*, as suggested by no significant effect on biomass.

P. edulis mesophyll cells showed typical structural markers of accelerated cell senescence (ACS) in response to O_3, such as chloroplast degeneration, reduced chloroplast size or irregular shape (Günthardt-Goerg and Vollenweider, 2007) and decreased protein cell content (Günthardt-Goerg et al., 1997; Günthardt-Goerg and Vollenweider, 2007; Vollenweider et al., 2013; Moura et al., 2018). The proteins accumulated in the chloroplasts and protoplast suggest that they may be enzymes linked to senescence processes, since hydrolytic enzymes are involved in the degradation of cellular components in senescent leaves (Diaz-Mendoza et al., 2016).

Reduction in number and size, and degradation of starch grains in the chloroplasts induced by ozone were also reported in other controlled experiments and were associated with accelerated senescence

Table 2
Mean, median and range between minimum and maximum values of biochemical markers in leaves of *P. edulis* exposed to three treatments of ozone (AA = ambient air, AA + O_3 × 1.5 = intermediate and AA + O_3 × 2.0 = elevated ozone levels) for 97 days: reduced (AsA), oxidized (DHA), total (totAA) ascorbic acid (mg/g^{-1} dw), redox potential of ascorbic acid (AsA/AsA + DHA), reduced (GSH), oxidized (GSSG), total (totG) glutathione (μmol/g^{-1} dw), redox potential of glutathione (GSH/GSH + GSSG), catalase (CAT, unit/g^{-1} dw), glutathione reductase (GR, unit/g^{-1} dw), ascorbate peroxidase (APX, unit/g^{-1} dw) superoxide dismutase (SOD, unit/g^{-1} dw), total sugars (mg/g^{-1} dw), starch (mg/g^{-1} dw), total flavonoids (%), carotenoids (CAR, mg/g^{-1} dw), chlorophylls *a*, *b* and *total* (Chl *a*, Chl *b*, Chl *total*, mg/g^{-1} dw), chlorophyll ratio (Chl *a*/*b*), hydroxyl radical (•OH, % 2′-deoxyribose oxidative degradation dw), superoxide (O_2•$^-$, nmol/g dw), hydrogen peroxide (H_2O_2, μmol/g dw), malondialdehyde (MDA, mM^{-1} dw) and hydroperoxide conjugated diene (HPCD μmol/g^{-1} dw). Different letters indicate significant differences between the treatments for each parameter median by Holm-Sidak test ($p < 0.05$), n = 3.

Biochemical markers	AA		AA + O_3 × 1.5		AA + O_3 × 2.0	
	Mean	Range	Mean	Range	Mean	Range
Pigments						
Chl *a*	0.50 b	0.38–0.63	0.56 b	0.38–0.71	0.63 a	0.48–0.75
Chl *b*	0.81 a	0.55–0.99	0.83 a	0.53–1.06	0.67 a	0.39–0.92
Chl *total*	1.31 a	0.98–1.58	1.39 a	0.99–1.68	1.30 a	0.94–1.68
Chl *a*/*b*	0.62 b	0.56–0.78	0.70 b	0.36–0.97	0.97 a	0.73–1.38
CAR	0.03 b	0.01–0.03	0.03 b	0.01–0.06	0.06 a	0.04–0.06
Primary and secondary metabolites						
Total sugars	86.76 a	70.06–120.98	101.70 a	83.41–139.58	101.16 a	82.24–118.65
Starch	52.19 b	29.46–77.06	73.97 a	52.80–86.60	48.02 b	34.78–90.66
Total flavonoids	0.20 c	0.18–0.21	0.28 b	0.27–0.29	0.32 a	0.31–0.33
Antioxidants						
AsA	1.51 b	1.24–2.37	2.14 a	1.50–2.83	3.03 a	2.61–3.34
DHA	0.62 b	0.22–1.80	0.86 a	0.25–1.63	0.50 a	0.15–1.02
totAA	2.13 b	1.55–3.33	3.00 a	2.80–3.47	3.53 a	3.17–3.84
AsA/AsA + DHA	0.73 a	0.45–0.89	0.71 a	0.47–0.91	0.85 a	0.73–0.95
GSH	23.56 b	11.93–38.96	32.76 a	20.33–47.06	54.60 a	31.14–114.26
GSSG	22.19 b	8.99–35.70	31.07 a	17.34–44.60	52.53 a	30.81–94.61
totG	45.75 b	20.92–74.67	63.83 a	54.73–79.47	107.13 a	61.95–208.88
GSH/GSH + GSSG	0.57 a	0.39–0.75	0.51 a	0.35–0.70	0.50 a	0.37–0.56
CAT	206.33 a	129.98–317.85	179.89 b	119.65–244.10	170.72 b	135.00–194.88
GR	0.83 a	0.10–1.70	0.28 b	0.08–0.60	0.21 b	0.05–0.53
APX	24.17 a	13.42–39.54	10.95 b	4.49–24.84	12.61 b	3.90–29.14
SOD	0.24 a	0.10–0.49	0.27 a	0.16–0.38	0.13 a	0.01–0.33
Reactive oxygen species						
•OH	47.27 a	44.19–50.20	49.32 a	42.26–53.97	47.71 a	40.02–54.48
O_2•$^-$	26.14 b	20.25–36.75	59.09 a	44.61–69.00	68.37 a	33.91–87.00
H_2O_2	65.29 b	58.11–69.77	76.01 a	58.84–96.94	76.42 a	71.17–86.63
Lipid peroxidation						
MDA	18.47 b	13.56–24.18	22.27 b	12.86–35.03	28.46 a	22.01–37.82
HPDC	0.62 b	0.55–0.78	0.70 b	0.36–0.97	0.97 a	0.73–1.38

(Bäck et al., 1999; Moura et al., 2018), and with the decline in the carboxylation efficiency (Oksanen et al., 2001). The reduction of starch grains in ozone-fumigated leaves suggest that less carbon was available for tissue repairing, production of antioxidants and growth (Bäck et al., 1999). However, we observed few alterations in the starch contents of the leaf tissues under high levels of ozone and we did not observe changes in the content of total sugars and in net photosynthesis and biomass production, indicating that changes in the structure of starch grains inside the chloroplasts did not affect the associated physiological processes.

The partial or total collapse of groups of cells frequently observed in the palisade parenchyma was also indicative of the programmed cell death (PCD) process following the ACS induced by O_3 in *P. edulis*. Increased ROS concentrations (as observed for hydrogen peroxide and superoxide in the present study) can cause rapid localized cell death, characterized by incomplete cellular degradation, altered cell membrane integrity and cell wall changes leading to cell collapse, processes that do not require energy (Günthardt-Goerg and Vollenweider, 2007). These cellular alterations indicate hypersensitive response-like (HR-like, similar to those induced by biotic stress) commonly found in O_3 fumigated species, including native vine species (Moura et al., 2011; Alves et al., 2016). We suggest that the deformation of the chloroplasts and the sinuous cell walls of palisade parenchyma were the first stages in the cell death process that culminated in the total collapse of groups of cells. In addition, cell collapse in the spongy parenchyma was also observed in the present study, although less frequently, mainly around the stomata. The same evidences were observed in the vine species *Ipomoea nil* under controlled conditions (Moura et al., 2011).

Hypertrophy and hyperplasia of the mesophyll cells were observed in studies that simulated the effect of acid rain on leaves (Silva et al., 2005; Sant'Anna-Santos et al., 2006). Although this is unusual, hypertrophy may also occur in the mesophyll in response to O_3 (Fink, 1999). We suggest that the hypertrophy and hyperplasia observed in mesophyll cells in *P. edulis* indicated acclimation to ozone. Both phenomena increase the compactness of the mesophyll layer, thus increasing the resistance to ozone diffusion. In addition, the increase of mesophyll compactness resulted in a higher leaf mass per area in leaves belonging to AA + O_3 × 2.0 treated plants, which can explain unchanged levels of biomass production among treatments in concomitance with reduction of RGR of leaves under high ozone.

Lipofuscin-like compounds were detected by confocal analyses in higher proportion inside the chloroplasts of leaf tissues from the high ozone treatment than in those from the AA treatment. Lipofuscins are liposoluble fluorescent products originating from the interaction of malonyl-dialdehyde with protein amino groups (Roshchina and Roshchina, 2003; Roshchina et al., 2015). Peak emission of this lipid peroxidation indicator was evidenced in pollen of *Passiflora caerulea* after 0.15 ppm–5 ppm h O_3 doses (Roshchina and Mel'nikova, 2001). In addition, the increased contents of MDA and HPDC in leaves from the O_3 × 2.0 treatment suggest that the lipid peroxidation resulted in ACS. In fact, these compounds are produced at the beginning and end of the lipid peroxidation chain, respectively. The ACS can be accelerated by an early onset of visible injury and also occurs in younger tissues, in response to increased ROS concentrations (Günthardt-Goerg and Vollenweider, 2007; Alves et al., 2016).

The increased hydrogen peroxide and superoxide leaf concentrations might also have stimulated antioxidant responses in *P. edulis* exposed to ozone, such as enhancement in the levels of flavonoids, ascorbic acid, glutathione and carotenoids. The constitutive flavonoids (of C-glycoside type) are one of the main bioactive compounds found in leaves of *P. edulis* (Ayres et al., 2015). We can assume that a great part of the increase in the leaf content of flavonoids came from the chloroplasts, based on the direct observation of in situ emission of these compounds by confocal laser scanning microscopy. The flavonoids located in the outer envelope membranes of the chloroplast (OEM) have antioxidant functions, limit the diffusion of ROS out of the chloroplast and preserve the outer membrane against oxidative damage (Roshchina and Roshchina, 2003; Agati et al., 2007, 2012). Besides, the biosynthesis of some flavonoids occurs inside of the chloroplasts (Agati et al., 2007).

Plants are equipped with an efficient antioxidant apparatus composed by antioxidant and non-enzymatic components which balance the cellular redox homeostasis and protect them against excessive ROS-triggered oxidative stress. The ascorbate-glutathione cycle ensures the regeneration of ascorbate by a sequence of redox reactions involving glutathione and nicotinamide adenine dinucleotide phosphate (NADPH) (Foyer and Noctor, 2011). The antioxidant power is not only limited to ascorbate and glutathione but also the antioxidant compounds such as superoxide dismutase, peroxidases and catalases (Caregnato et al., 2008). Under favorable conditions, a fully-functional antioxidant machinery maintains the redox balance with plant cells. However, enhancement of ROS generation promoted by different environmental cues, such as ozone, can lead to the alteration of redox balance, this promoting oxidative stress events (Bray et al., 2000).

In addition to ROS scavenging promoted by ascorbate-glutathione components, other secondary metabolites with a strong free-radical-scavenging ability can sensibly participate in ROS controlling in leaves, these including flavonoids (Agati et al., 2013).

A decrease in the activity of APX in the chloroplasts may be followed by an increase in the levels of flavonoids to control ROS propagation. This response was observed in the plants of *P. edulis* exposed to high ozone concentrations. Flavonoids like rutin and quercetin are also scavengers of superoxide anions (Yuting et al., 1990) and for this reason they may act in place of SOD thereby explaining the decrease of the activity of this enzyme in leaf samples of *P. edulis*. SOD catalyzes the dismutation of the superoxide radical in H_2O_2 and H_2O in the presence of proton H^+ (Scandalios, 1993). In foliar samples of *P. edulis* the increment of H_2O_2 suggests the inhability of CAT and APX to control the level of H_2O_2 generated by the superoxide anion scavenging ability orchestrated by flavonoids and SOD activity. Flavonoids are capable of inhibiting glutathione reductase (Elliot et al., 1992) which also could explain the decrease of activity of this enzyme in leaf samples of *P. edulis*. Although some studies (e.g. Furlan et al., 2010; Santos and Furlan, 2013) reported an increase in the concentrations of flavonoids in plants exposed to ozone, none of them related this enhancement with the induction of OEM flavonoids. Foliar levels of other non-enzymatic antioxidants (ascorbic acid and glutathione) were enhanced in plants exposed to the AA + O_3 × 1.5 and AA + O_3 × 2.0 treatments, respectively, when compared to plants grown in AA. The high leaf contents of ascorbic acid and glutathione, as well as their high and stable redox potential, as indicated by the ratio between their reduced and total forms (AsA/AsA + DHA; GSH/GSH + GSSG), were key responses for maintaining high redox equilibrium in *P. edulis* under ozone, although enhanced lipid peroxidation or MDA by-products were observed in plants exposed to the highest ozone concentrations. In our experiment the increment of AsA and the higher AsA/AsA + DHA suggest that *P. edulis* plants were able to efficiently regenerate the oxidized DHA to reduced AsA which is the biological active form of ascorbate capable of ROS scavenging (Burkey et al., 2006), this support the O_3 tolerance of *P. edulis*. Similar results were obtained for other species, under either experimental or natural conditions (e.g. Burkey et al., 2006; Aguiar-Silva et al., 2016; Esposito et al., 2016; Brandão et al., 2017). The high levels of carotenoids, observed inside the chloroplasts in plants fumigated with high ozone, can be also considered biochemical responses associated to the high tolerance of *P. edulis* against environmental oxidative stressors. Carotenoids are natural pigments mostly responsible for the yellow, orange and red color of the fruits (Da Silva et al., 2014), being z-carotene identified as the predominant compound in passion fruit (Pertuzatti et al., 2015). Carotenoids are essential for the correct assembly and functioning of photosystems and protect from photo-oxidative damage preventing and quenching ROS generated from triplet excited chlorophylls via xanthophyll cycle (Esteban et al., 2015). While non-enzymatic antioxidants generally showed higher concentration in the ozone-addition treatments, the enzymatic activity of CAT, APX and GR decreased at the elevated ozone treatment (O_3 × 2.0). The lowest activity level of these enzymes in plants from this treatment coincided with the highest contents of ascorbic acid and glutathione, showing that the ascorbate–glutathione cycle of *P. edulis* was stimulated in response to O_3. Dafré-Martinelli et al. (2011) analyzed the redox state of the vine *Ipomoea nil* 'Scarlet O'Hara' growing under O_3 in an urban area in Brazil, and concluded that ascorbic acid and glutathione were crucial for increasing plant tolerance to ozone.

5. Conclusions

Exposure to high levels of O_3 did not significantly affect the content of total sugars, net photosynthesis, growth parameters (diameter and height) and biomass production. *P. edulis* showed several reactive mechanisms against the effects of O_3, such an effective enhancement antioxidant system, principally consisting of non-enzymatic antioxidants (ascorbic acid, carotenoids, glutathione and flavonoids located in the outer envelope membranes of the chloroplast), hyperplasia and hypertrophy of the mesophyll cells (thus reducing the intercellular space and increasing the resistance to ozone diffusion), and accelerated cell senescence which may have accelerated leaf abscission and thus reduced the number of leaves per plant. So, these leaf traits indicate *P. edulis* as tolerant to the oxidative stress caused by O_3.

Acknowledgments

The authors thank the financial support provided by Fundação de Desenvolvimento da Pesquisa do Agronegócio (FUNDEPAG), Coordenação de Aperfeiçoamento de Pessoal de Nível Superior (CAPES), Conselho Nacional de Desenvolvimento Científico e Tecnológico (CNPq), the Fondazione Cassa di Risparmio di Firenze (2013/7956) and the LIFE15 ENV/IT/000183 project MOTTLES. We also thank Alessandro Materassi for design and maintenance of the ozone FACE, Moreno Lazzara for assistance during the field work, Adriana Matsukuma and Wilton Lima for assistance with confocal microscopy at Central Analítica (Instituto de Química, USP).

Appendix A. Supplementary data

Supplementary data to this article can be found online at https://doi.org/10.1016/j.scitotenv.2018.11.425.

References

Agati, G., Matteini, P., Goti, A., Tattini, M., 2007. Chloroplast-located flavonoids can scavenge singlet oxygen. New Phytol. 174, 77–89.
Agati, G., Azzarello, E., Pollastri, S., Tattini, M., 2012. Flavonoids as antioxidants in plants: location and functional significance. Plant Sci. 196, 67–76.
Agati, G., Brunetti, C., Ferdinando, M., Ferrini, F., Pollastri, S., Tattini, M., 2013. Functional roles of flavonoids in photoprotection: new evidence, lessons from the past. Plant Physiol. Biochem. 72, 35–45.
Aguiar-Silva, C., Brandão, S.E., Domingos, M., Bulbovas, P., 2016. Antioxidant responses of Atlantic Forest native tree species as indicators of increasing tolerance to oxidative stress when they are exposed to air pollutants and seasonal tropical climate. Ecol. Indic. 63, 154–164.

Alexieva, V., Sergiev, I., Mapelli, S., Karanov, E., 2001. The effect of drought and ultraviolet radiation on growth and stress markers in pea and wheat. Plant Cell Environ. 24, 1337–1344.

Alves, E.S., Moura, B.B., Pedroso, A.N.V., Tresmondi, F., Machado, S.R., 2016. Cellular markers indicative of ozone stress on bioindicator plants growing in a tropical environment. Ecol. Indic. 67, 417–424.

Amaral, L.I.V., Costa, P.M.F., Aidar, M.P.M., Gaspar, M., Buckeridge, M.S., 2007. Novo método enzimático rápido e sensível de extração e dosagem de amido em materiais vegetais. Hoehnea 34, 425–431.

Amorim, T.A., Nunes-Fretiras, A.F., Rosado, B.H.P., 2018. Revisiting the hypothesis for increasing liana abundance in seasonal forest: a theoretical review. Plant Soil 430, 1–6.

Araújo, M.H., Silva, I.C.V., Oliveira, P.F., Barreto, A.R.R., Konnod, T.U.P., Esteves, F.A., Bartha, T., Aguire, F.A., Lopes, N.P., Dermenjianf, R.K., Guimarães, D.O., Leala, I.C.R., Lasunskaiab, E.B., Muzitanoa, M.F., 2017. Biological activities and phytochemical profile of *Passiflora mucronata* from the Brazilian restinga. Rev. Bras. Farmacogn. 27, 702–710.

Ashmore, M.R., 2005. Assessing the future global impacts of ozone on vegetation. Plant Cell Environ. 28, 949–964.

Ayres, A.S.F.S.J., Araújo, L.L.S., Soares, T.C., Costa, G.M., Reginatto, F.H., Ramos, F.A., Castellanos, L., Schenkel, E.P., Soares-Rachetti, V.P., Zucolotto, S.M., Gavioli, E.C., 2015. Comaprative central effects of the aqueous leaf extract of two populations of *Passiflora edulis*. Rev. Bras. Farmacogn. 25, 499–505.

Azevedo, R.A., Alas, R.M., Smith, R.J., Lea, P.J., 1998. Response of antioxidant enzymes to transfer from elevated carbon dioxide to air and ozone fumigation in the leaves and roots of wild-type and a catalase deficient mutant of barley. Physiol. Plant. 104, 280–292.

Bäck, J., Vanderklein, D.W., Topa, M.A., 1999. Effects of elevated ozone on CO_2 uptake and leaf structure in sugar maple under two light environments. Plant Cell Environ. 22, 137–147.

Benincasa, M.M.P., 1988. Análise de crescimento de plantas: noções básicas. 2° edição. Funep, Jaboticabal, p. 41.

Bhaduri, A.M., Fulekar, M.H., 2012. Assessment of arbuscular mycorrhizal fungi on the phytoremediation potential of *Ipomoea aquatica* on cadmium uptake. 3 Biotech 2, 193–198.

Brandão, S.E., Bulbovas, P., Lima, M.E., Domingos, M., 2017. Biochemical leaf traits as indicators of tolerance potential in tree species from the Brazilian Atlantic Forest against oxidative environmental stressors. Sci. Total Environ. 575, 406–417.

Bray, E.A., Baylei-Serres, J., Werentilnyk, E., 2000. Responses to abiotic stress. In: Buchanan, B.B., Gruissem, W., Jones, R.L. (Eds.), Biochemistry and Molecular Biology of Plants. American Society of Plant Physiologists, USA, New York, pp. 1158–1203.

Burkey, K.O., Neufeld, H.S., Souza, L., Chappelka, A.H., Davison, A.W., 2006. Seasonal profiles of leaf ascorbic acid content and redox state in ozone-sensitive wildflowers. Environ. Pollut. 143, 427–434.

Caregnato, F.F., Koller, C.E., MacFarlane, G.R., Moreira, J.C.F., 2008. The glutathione antioxidant system as a biomarker suite for the assessment of heavy metal exposure and effect in the grey mangrove, *Avicennia marina* (Forsk.) Vierh. Mar. Pollut. Bull. 56, 1119–1127.

Castro, P.C.F., Hoshino, A., Silva, J.C., Mendes, F.R., 2007. Possible anxiolytic effect of two extracts of *Passiflora quadrangularis* L. in experimental models. Phytother. Res. 21, 481–484.

CLRTAP, 2017. Mapping critical levels for vegetation, chapter III of manual on methodologies and criteria for modelling and mapping critical loads and levels and air pollution effects, risks and trends. UNECE Convention on Long-range Transboundary Air Pollution On web at. www.icpmapping.org, Accessed date: 27 July 2018.

Da Silva, L.M.R., de Figueiredo, E.A.T., Ricardo, N.M.P.S., Vieira, I.G.P., de Figueiredo, R.W., Brasil, I.M., Gomes, C.L., 2014. Quantification of bioactive compounds in pulps and by-products of tropical fruits from Brazil. Food Chem. 143, 398–404.

Dafré-Martinelli, M., Nakazato, R.K., Dias, A.P.L., Rinaldi, M.C.S., Domingos, M., 2011. The redox state of *Ipomoea nil* 'Scarlet O'Hara' growing under ozone in a subtropical area. Ecotoxicol. Environ. Saf. 74, 1645–1652.

D'Andrea, L., Amenos, M., Rodriguez-Concepcion, M., 2014. Confocal Laser Scanning Microscopy detection of chlorophylls and carotenoids in chloroplasts and chromoplasts of tomato fruit. In: Rodriguez-Concepcion, M. (Ed.), Plant Isoprenoids: Methods and Protocols. Springer, New York, pp. 227–232.

DeWalt, S.J., Chave, J., 2004. Structure and biomass of four lowland Neotropical forests. Biotropica 36, 7–19.

Dhawan, K., Dhawan, S., Sharma, A., 2004. Passiflora: a review update. J. Ethnopharmacol. 94, 1–23.

Diaz-Mendoza, M., Velasco-Arroyo, B., Santamaria, M.E., González-Melendi, P., Martinez, M., Diaz, I., 2016. Plant senescence and proteolysis: two processes with one destiny. Genet. Mol. Biol. 39, 329–338.

Dornelas, M.C., Fonseca, T.C., Rodriguez, A.P.M., 2006. Brazilian passion flowers and novel passionate tropical flowering gems. Floriculture, Ornamental and Plant Biotechnology. Global Science Books, London.

Dubois, M., Gilles, A., Hamilton, J.K., Rebers, P.A., Smith, F., 1956. Colorimetric method for determination of sugars and related substances. Anal. Chem. 28, 350–355.

Eijckelhoff, C., Dekker, J.P., 1997. A routine method to determine the chlorophyll a, pheophytin a and β-carotene contents of isolated photosystem II reaction center complexes. Photosynth. Res. 52, 69–73.

Elliot, A.J., Scheiber, S.A., Thomas, C., Pardini, R.S., 1992. Inhibition of glutathione reductase by flavonoids: a structure-activity study. Biochem. Pharmacol. 44 (8), 1603–1608.

Esposito, M.P., Pedroso, A.N.V., Domingos, M., 2016. Assessing redox potential capacity of a native tree from the Atlantic Rain Forest in SE–Brazil during the exchange of the power generation source of an oil refinery. Sci. Total Environ. 550, 861–870.

Esposito, M.P., Nakazato, R.K., Pedroso, A.N.V.P., Lima, M.E.L., Figueiredo, M.A., Diniz, A.P., Kozovitz, A.R., Domingos, M., 2018. Oxidant-antioxidant balance and tolerance against oxidative stress in pioneer and non-pioneer tree species from the remaining Atlantic Forest. Sci. Total Environ. 625, 382–393.

Esteban, R., Barrutia, O., Artetxe, U., Fernández-Marin, B., Hernández, A., García-Plazaola, J.I., 2015. Internal and external factors affecting photosynthetic pigment composition in plants: a meta-analytical approach. New Phytol. 206, 268–280.

Feder, N., O'Brien, 1968. Plant microtechnique: some principles and new methods. Am. J. Bot. 55, 123–142.

Fernandes, F.F., Cardoso-Gustavson, P., Alves, E.S., 2016. Synergism between ozone and light stress: structural responses of polyphenols in a woody Brazilian species. Chemosphere 155, 573–582.

Ferreira, M.L., Esposito, J.B.N., Souza, S.R., Domingos, M., 2012. Critical analysis of the potential of *Ipomoea nil* Scarlet O'Hara for ozone biomonitoring in the sub-tropics. J. Environ. Monit. 14, 1959–1967.

Fink, S., 1999. Pathological and regenerative plant anatomy. Encyclopedia of Plant Anatomy vol. XIV/6. Gebrüder Bornträger, Berlin, Stuttgart, pp. 523–527.

Flora do Brasil 2020, d. Jardim Botânico do Rio de Janeiro.Available at:. http://floradobrasil.jbrj.gov.br/, Accessed date: May 2018 (under construction).

Foyer, C.H., Noctor, G., 2011. Ascorbate and glutathione: the heart of the redox hub. Plant Physiol. 155, 2–18.

Furlan, C.M., Santos, D.Y.A.C., Motta, L.B., Domingos, M., Salatino, A., 2010. Guava flavonoids and the effects of industrial air pollutants. Atmos. Pollut. Res. 1, 30–35.

Gahan, P.B., 1984. Plant Histochemistry and Cytochemistry. Academic Press, London.

Gowin, T., Goral, I., 1977. Chlorophyll and pheophytins content in needles of different age of trees growing under conditions of chronic industrial pollution. Acta Soc. Bot. Pol. 46, 151–159.

Günthardt-Goerg, M.S., Vollenweider, P., 2007. Linking stress with macroscopic and microscopic leaf response in trees: new diagnostic perspectives. Environ. Pollut. 147, 467–488.

Günthardt-Goerg, M.S., McQuattie, C.J., Scheidegger, C., Rhiner, C., Matyssek, R., 1997. Ozone-induced cytochemical and ultrastructural changes in leaf mesophyll cell. Can. J. For. Res. 27, 453–463.

Hernandez-Gimenez, M.J., Lucas, M.M., de Felipe, M.R., 2002. Antioxidant defense and damage in senescing lupin nodules. Plant Physiol. Biochem. 40, 645–657.

Hodges, D.M., DeLong, J.M., Forney, C.F., Prange, R.K., 1999. Improving the thiobarbituric acid-reactive-substances assay for estimating lipid peroxidation in plant tissues containing anthocyanin and other interfering compounds. Planta 207, 604–611.

Hoshika, Y., Moura, B., Paoletti, E., 2018. Ozone risk assessment in three oak species as affected by soil water availability. Environ. Sci. Pollut. Res. 25, 8125–8136.

Israr, M., Sahi, S., Datta, R., Sarkar, D., 2006. Bioaccumulation and physiological effects of mercury in Sesbania drummondii. Chemosphere 65, 591–598.

Jarvis, P.G., 1976. Interpretation of variations in leaf water potential and stomatal conductance found in canopies in field. Philos. Trans. R. Soc. Lond. B 273, 593–610.

Kanofsky, J.R., Sima, P.D., 2005. Assay for singlet oxygen generation by plant leaves exposed to ozone. Methods Enzymol. 319, 512–520.

Kivimäenpää, M., Jonsson, A.M., Stjernquist, I., Sellden, G., Sutinen, S., 2004. The use of light and electron microscopy to assess the impact of ozone on Norway spruce needles. Environ. Pollut. 127, 441–453.

Kraus, T.E., Evans, R.C., Fletcher, R.A., Paul, S.K.P., 1995. Paclobutrazol enhances tolerance to increased levels of UV-B radiation in soybean (*Glycine max*) seedlings. Can. J. Bot. 73, 797–806.

Landi, M., 2017. Commentary to: "Improving the thiobarbituric acid-reactive-substances assay for estimating lipid peroxidation in plant tissues containing anthocyanin and other interfering compounds". Planta 245 (6), 1097.

Levin, A.G., Pignata, M.L., 1995. *Ramalina ecklonii* as a bioindicator of atmospheric pollution in Argentina. Can. J. Bot. 73, 1196–1202.

Lodovici, M., Bigagli, E., 2011. Oxidative stress and air pollution exposure. J. Toxicol. 2011, 1–9.

Lopes, G.K.B., Schulman, H.M., Hermes-Lima, M., 1999. Polyphenol tannic acid inhibits hydroxyl radical formation from Fenton reaction by complexing ferrous ions. Biochim. Biophys. Acta 1472, 142–152.

López, A., Montaño, A., Garcia, P., Garrido, A., 2005. Note: quantification of ascorbic acid and dehydroascorbic acid in fresh olives in commercial presentations of table olives. Food Sci. Technol. Int. 11, 199–204.

Manning, W.J., Godzik, B., 2004. Bioindicator plants for ambient ozone in Central and Eastern Europe. Environ. Pollut. 130, 33–39.

Matyssek, R., Sandermann, H., 2003. Impact of ozone on trees: an ecophysiological perspective. Prog. Bot. 64, 349–404.

Matyssek, R., Wieserb, G., Calfapietra, C., de Vriesd, W., Dizengremelf, P., Ernst, D., Jolivet, Y., Mikkelsen, T.N., Mohren, G.M.J., Le Thiec, D., Tuovinen, J.P., Weatherall, A., Paoletti, E., 2012. Forests under climate change and air pollution: gaps in understanding and future directions for research. Environ. Pollut. 160, 57–65.

Moura, B.B., Souza, S.R., Alves, E.S., 2011. Structural responses of *Ipomoea nil* (L.) Roth "Scarlet O'Hara" (Convolvulaceae) exposed to ozone. Acta Bot. Bras. 25, 122–129.

Moura, B.B., Hoshika, Y., Ribeiro, R.V., Paoletti, E., 2017. Exposure- and flux-based assessment of ozone risk to sugarcane plants. Atmos. Environ. 176, 252–260.

Moura, B.B., Alves, E.S., Marabesi, M.A., Souza, S.R., Schaub, M., Vollenweider, P., 2018. Ozone affects leaf physiology and causes injury to foliage of native tree species from the tropical Atlantic forest of southern Brazil. Sci. Total Environ. 610–611, 912–925.

Ocampo, J., d'Eeckenbrugge, G.C., Jarvis, A., 2010. Distribution of the genus *Passiflora* L. diversity in Colombia and its potential as an indicator for biodiversity management in the coffee growing zone. Diversity 2, 1158–1180.

Oksanen, E., Sober, J., Karnosky, D.F., 2001. Impacts of elevated CO_2 and/or O_3 on leaf ultrastructure of aspen (*Populus tremuloides*) and birch (*Betula papyrifera*) in the aspen FACE experiment. Environ. Pollut. 115, 437–446.

Otobone, F.J., Martins, J.V.C., Trombelli, M.A., Andreatini, R., Audi, E.A., 2005. Anxiolytic and sedative effects of a combined extract of *Passiflora alata* Dryander and *Valeriana officinalis* L. in rats. Acta Sci. Health Sci. 27, 145–150.
Paoletti, E., Materassi, A., Fasano, G., Hoshika, Y., Carriero, G., Silaghi, D., Badea, O., 2017. A new-generation 3D ozone FACE (Free Air Controlled Exposure). Sci. Total Environ. 575, 1407–1414.
Pell, E.J., Schlagnhaufer, C.D., Arteca, R.N., 1997. Ozone-induced oxidative stress: mechanisms of action and reaction. Physiol. Plant. 100, 264–273.
Pérez-Salicrup, D.R., Schnitzer, S.A., Putz, F.E., 2004. The community ecology and management of lianas. For. Ecol. Manag. 190, 1–2.
Pertuzatti, P.B., Sganzerla, M., Jacques, A.C., Barcia, M.T., Zambiazi, R.C., 2015. Carotenoids, tocopherols and ascorbic acid contente in yellow passion fruit (*Passiflora edulis*) grown under different cultivation systems. LTW Food Sci. Technol. 64, 259–263.
Phillips, O.L., Martinez, R.V., Arroyo, L., Baker, T.R., Killeen, T., Lewis, S.L., Malhi, Y., Mendoza, A.M., Neill, D., Vargas, P.N., Alexiades, M., Cerón, C., Di Fiore, A., Erwin, T., Jardim, A., Palacios, W., Saldias, M., Vinceti, B., 2002. Increasing dominance of large lianas in Amazonian forests. Nature 418, 770–774.
Pivello, V.R., Vieirab, M.V., Grombone-Guaratinic, M.T., Matos, D.M.S., 2018. Thinking about super-dominant populations of native species – examples from Brazil. Perspect. Ecol. Conserv. 16, 74–82.
Puckette, M.C., Weng, H., Mahalingam, R., 2007. Physiological and biochemical responses to acute ozone-induced oxidative stress in *Medicago truncatula*. Plant Physiol. Biochem. 45, 70–79.
Reddy, A.R., Chaitanya, K.V., Jutur, P.P., Sumithra, K., 2004. Differential antioxidative responses to water stress among five mulberry (*Morus alba* L.) cultivars. Environ. Exp. Bot. 52, 33–42.
Roshchina, V.V., 2008. Fluorescing World of Plant Secreting Cells. Science Publishers, Enfields.
Roshchina, V.V., Mel'nikova, E.V., 2001. Pollen chemosensitivity to ozone and peroxides. Russ. J. Plant Physiol. 48, 74–83.
Roshchina, V.V., Roshchina, V.D., 2003. Ozone and Plant Cell. Kluwer Academic Publishers, Dordrecht.
Roshchina, V.V., Yashin, V.A., Kuchin, A.V., 2015. Fluorescent analysis for bioindication of ozone on unicellular models. J. Fluoresc. 25, 595–601.
Rossell, I.M., Eggleston, H., 2017. Elevational distribution of temperate lianas along trails in Pisgah National Forest. Southeast. Nat. 16, 443–450.
Sá, A.F.L., Valeri, S.V., Cruz, M.C.P., Barbosa, J.C., Rezende, G.M., Teixeira, M.P., 2014. Effects of potassium application and soil moisture on the growth of *Corymbia citriodora* plants. Cerne 20, 645–651.
Saitanis, C.J., 2003. Background ozone monitoring and phytodetection in the greater rural area of Corinth-Greece. Chem. Aust. 51, 913–923.
Sant'Anna-Santos, B.F., Silva, L.C., Azevedo, A.A., Aguiar, R., 2006. Effects of simulated acid raind on leaf anatomy and micromorphology of *Genipa americana* L. (Rubiaceae). Braz. Arch. Biol. Technol. 49, 313–332.
Santos, A.C.R., Furlan, C.M., 2013. Levels of phenolic compounds in *Tibouchina pulchra* after fumigation with ozone. Atmos. Pollut. Res. 4, 250–256.
Scandalios, J.G., 1993. Oxygen stress and superoxide dismutases. Plant Physiol. 101, 7–12.
Scherer, C.C., 2014. Conservação filogenética de nicho climático para espécies do gênero *Passiflora* L. (Passifloraceae) com ocorrência no Brasil. Universidade Federal do Paraná, Curitiba (M.Sc. thesis).
Schnitzer, S.A., 2005. A mechanistic explanation for global patterns of liana abundance and distribution. Am. Nat. 166, 262–276.
Schnitzer, S.A., Bongers, F., 2002. The ecology of lianas and their role in forests. Trends Ecol. Evol. 17, 223–230.
Silva, L.D., Oliva, M.A., Azevedo, A.A., Araújo, J.M., Aguiar, R.M., 2005. Micromorphological and anatomical alterations caused by simulated acid rain in Restinga plants: *Eugenia uniflora* and *Clusia hilariana*. Water Air Soil Pollut. 168, 129–143.
Soja, G., Eid, M., Gangl, H., Redl, H., 1997. Ozone sensitivity of grapevine (*Vitis vinifera* L.): evidence for a memory effect in a perennial crop plant? Phyton 37, 265–270.
Souza, P.U., Lima, L.K.S., Soaresb, T.L., Jesus, O.N., Filho, M.A.C., Girardi, E.A., 2018. Biometric, physiological and anatomical responses of *Passiflora* spp. to controlled water deficit. Sci. Hortic. 229, 77–90.
Vollenweider, P., Ottiger, M., Günthardt-Goerg, M.S., 2003. Validation of leaf ozone symptoms in natural vegetation using microscopical methods. Environ. Pollut. 124, 101–118.
Vollenweider, P., Fenn, M.E., Menard, T., Günthardt-Goerg, M., Bytnerowicz, A., 2013. Structural injury underlying mottling in ponderosa pine needles exposed to ambient ozone concentrations in the San Bernardino Mountains near Los Angeles, California. Trees 27, 895–911.
Wang, A.G., Luo, G.H., 1990. Quantitative relation between the reaction of hydroxylamine and superoxide anion radicals in plants. Plant Physiol. Commun. 6, 55–57.
Wetzel, S., Demmers, C., Greenwood, J.S., 1989. Spherical organelles, analogous to seed protein bodies, fluctuate seasonally in parenchymatous cell of hardwoods. Can. J. Bot. 67, 3439–3445.
Wintermans, J.F.G.M., De Mots, A., 1965. Spectrophotometric characteristics of chlorophylls *a* and *b* and their phenophytins in ethanol. Biochim. Biophys. Acta 109 (2), 448–453.
Wohlmuth, H., Penman, K.G., Pearson, T., Lehmann, R.P., 2010. Pharmacognosy and chemo types of passionflower (*Passiflora incarnata* L.). Biol. Pharm. Bull. 33, 1015–1018.
Xu, H., Vavilin, D., Vermaas, W., 2001. Chlorophyll *b* can serve as the major pigment in functional photosystem II complexes of cyanobacteria. Proc. Natl. Acad. Sci. U. S. A. 98, 14168–14173.
Yudasheva, L.N., Carvalho, E.B., Castanho, M.T.J.A., Krasilnikov, O.V., 2005. Cholesterol-dependent hemolytic activity of *Passiflora quadrangularis* leaves. Braz. J. Med. Biol. Res. 38, 1061–1070.
Yuting, C., Rongliang, Z., Zhongjian, J., Yong, J., 1990. Flavonoids as superoxide scavengers and antioxidants. Free Radic. Biol. Med. 9 (1), 19–21.